

AD-A010 205

IONOSPHERIC MODELING

L. R. McGill

Utah State University

Prepared for:

Advanced Research Projects Agency

30 June 1974

DISTRIBUTED BY:

**NTIS**

National Technical Information Service  
U. S. DEPARTMENT OF COMMERCE

157057

Final Report

IONOSPHERIC MODELING

Center for Research in Aeronomy  
Utah State University  
Logan, Utah 84322

L. R. McGill, Principal Investigator  
(801) 752-4100 Ext. 7879

Contract Number: N00014-67-A-0220-0004

ARPA Order Number: 2266/8-11-72

Program Code Number: 4B969

Ending Date: 30 June 1974

\$94,101

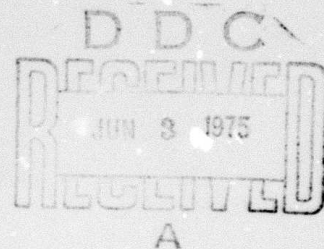
Scientific Officer: Director, Physics Program  
Physical Sciences Division  
Office of Naval Research  
Department of the Navy  
800 North Quincy Street  
Arlington, Virginia 22217

Sponsored by  
Advanced Research Projects Agency

ARPA Order No. 2266

The views and conclusions contained in this document are those of the authors and should not be interpreted as necessarily representing the official policies, either expressed or implied, of the Advanced Research Projects Agency or the U. S. Government.

Reproduced by  
NATIONAL TECHNICAL  
INFORMATION SERVICE  
U.S. Department of Commerce  
Springfield, VA. 22151



DISTRIBUTION STATEMENT A

Approved for public release;  
Distribution Unlimited

ADA010205

1.

The work accomplished under this contract was directed toward the development of a theoretical computer-oriented model of the polar ionosphere between the heights of 50 and 500 km. This model was based on first principles of atmospheric physics, except where the physical processes were not understood. The model was to be comprehensive enough to predict both the "quiet" and "disturbed" polar ionospheric conditions. Our strategy for solving these problems was to model the "quiet" ionosphere first by separating the total height region into the E and F regions (100-500 km) and the D region (50-100 km). This was done because the physical processes are much different above and below 100 km.

#### E and F Regions

The E and F regions of the polar ionosphere are similar to those at mid-latitudes except for energetic particle precipitation down the geomagnetic field lines. To handle the kinetic processes, we modified a chemical-kinetics computer program developed by Adams and Megill [1970]. This computer code allows as many as 31 species to interact in up to 51 different reactions with 15 separate photoreactions. The flow diagram of the modified computer program is given in Figure 1. The processes indicated in the dashed areas were not implemented before termination of the contract.

Photoionization rates during the daytime for  $O_2^+$ ,  $N_2^+$ ,  $O^+$ , and  $NO^+$  are calculated by utilizing the approximations to the Chapman function for optical depth derived by Swider [1964]. During the daytime the photoionization rates are three orders of magnitude greater than

1.a

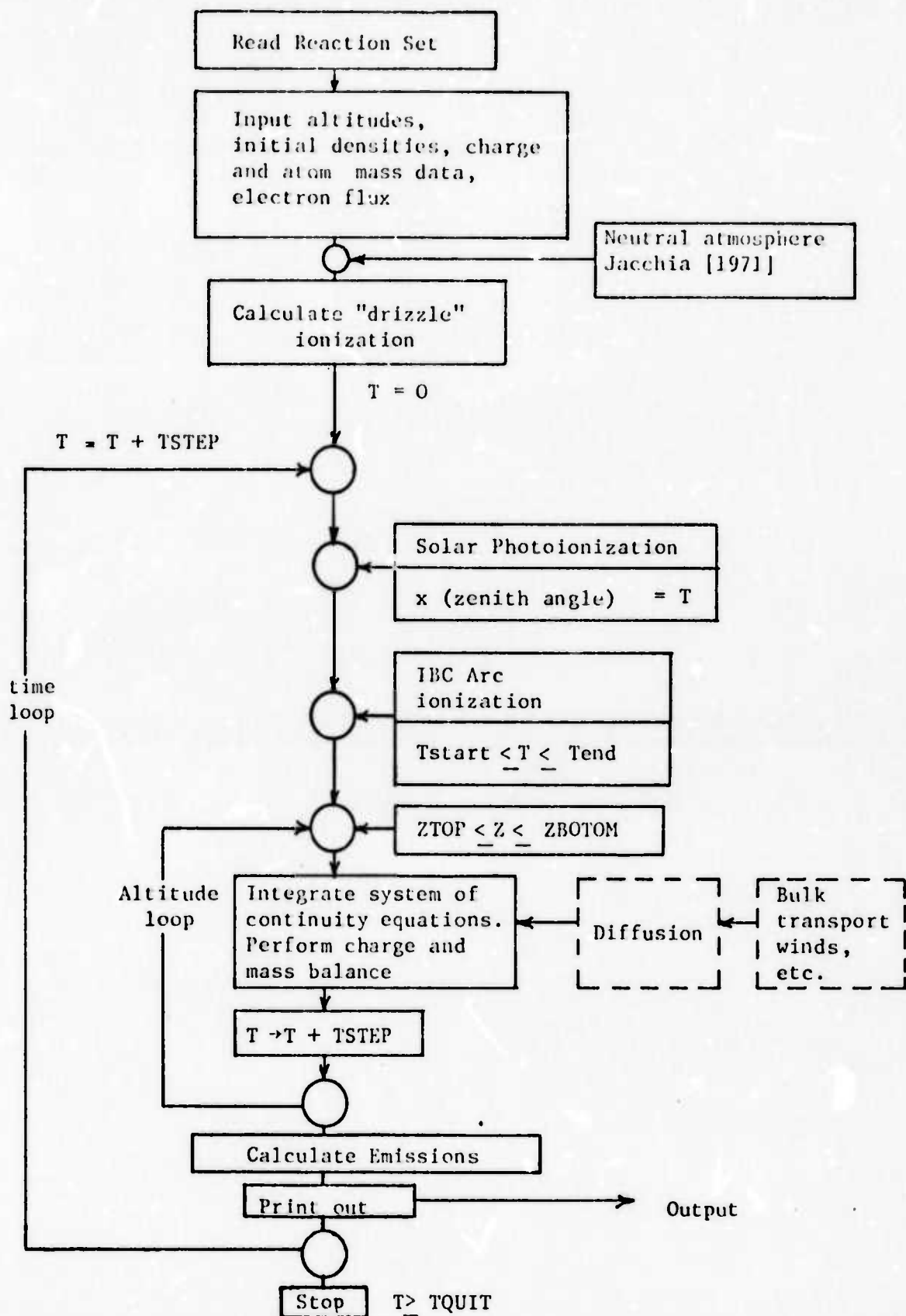


Figure 1

the ionization produced by the precipitation "drizzle" electron flux. See Figure 2. The nighttime ionization in the polar ionosphere is a complicated mixture of energetic particles and scattered solar radiation. The mid-latitude E region is maintained at a level of  $10^3$ - $10^4$  electrons/cm<sup>3</sup> through the night by solar radiation scattered to the dark side of the earth by the earth's hydrogen and helium geocorona. The model of Ogawa and Tohmatsu [1967] was utilized even though the ionization rate from scattered light is a function of the radiation-transport geometry [Meier, 1974]. Comparison of the production rates due to scattered radiation, Figure 3, and drizzle flux, Figure 2, show that these two processes are about the same in the nighttime polar ionosphere. Electron precipitation was divided into a quiet "drizzle" flux and into 3 strengths of auroral arc precipitation. The "drizzle" precipitation is that found in the quiet auroral oval and in the polar cap [Burch, 1968]. The auroral arc precipitation was designated IBC-I, II and III, and defined as having flux values of  $10^7 \exp(-E/3.5)$ ,  $10^8 \exp(-E/8.5)$ , and  $10^9 \exp(-E/12.5)$  electrons per cm<sup>2</sup>-sec-ster-kev where E is the particle energy in kilo-electron volts. The production rates for N<sub>2</sub><sup>+</sup>, O<sub>2</sub><sup>+</sup> and O<sup>+</sup> due to electron fluxes is given by

$$Q_i(h) = \frac{\sigma_i N_i}{\sigma_{N_2} N_{N_2} + \sigma_{O_2} N_{O_2} + \sigma_O N_O} Q(h) \text{ (cm}^{-3} \text{ sec}^{-1}) \quad i=N_2, O_2 \text{ or } O$$

where Q(h) is the integral over all energies of the ionization rate



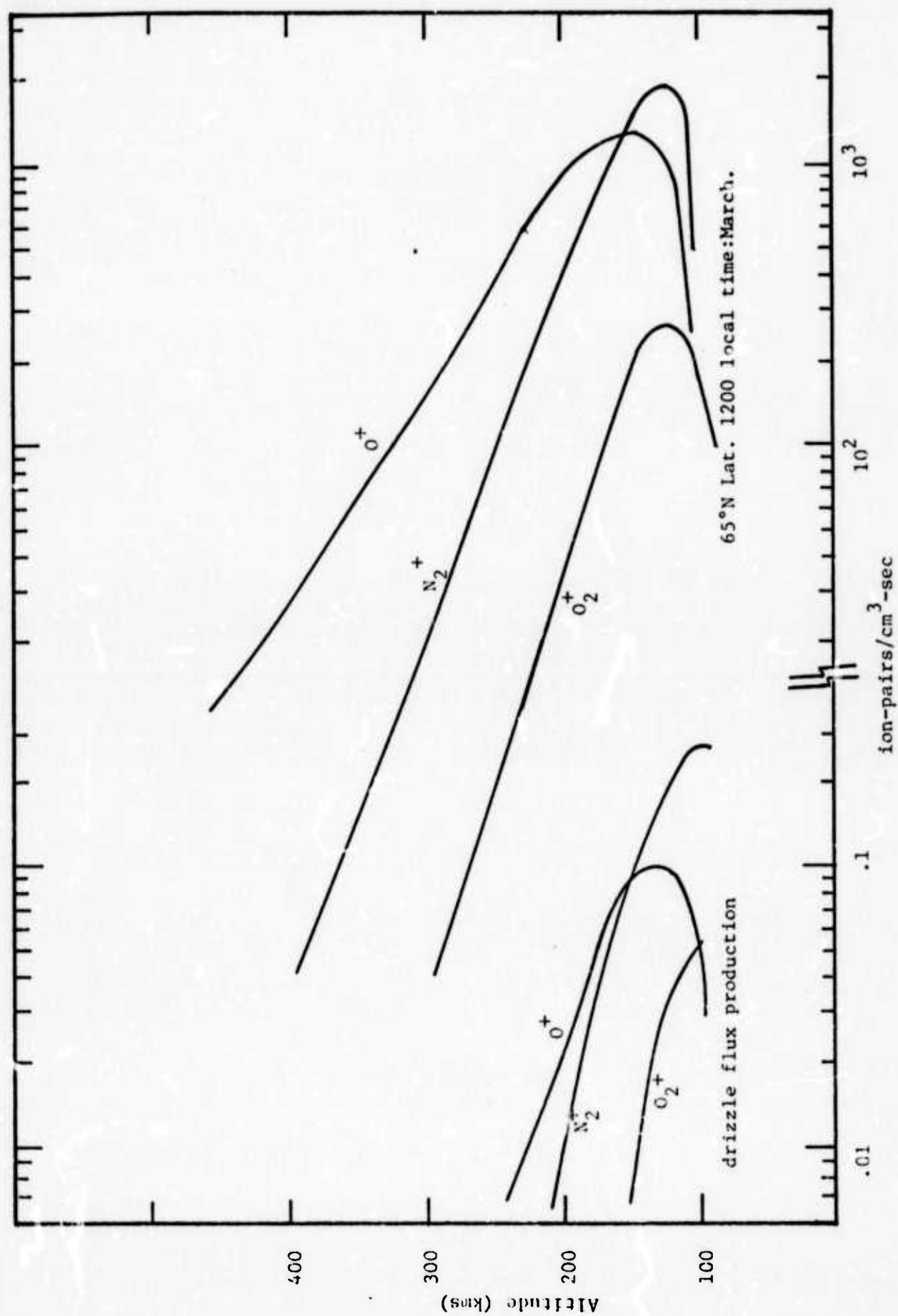


Figure 2. Ion Production Rates from Solar Radiation and "Drizzle" Precipitation Electrons.

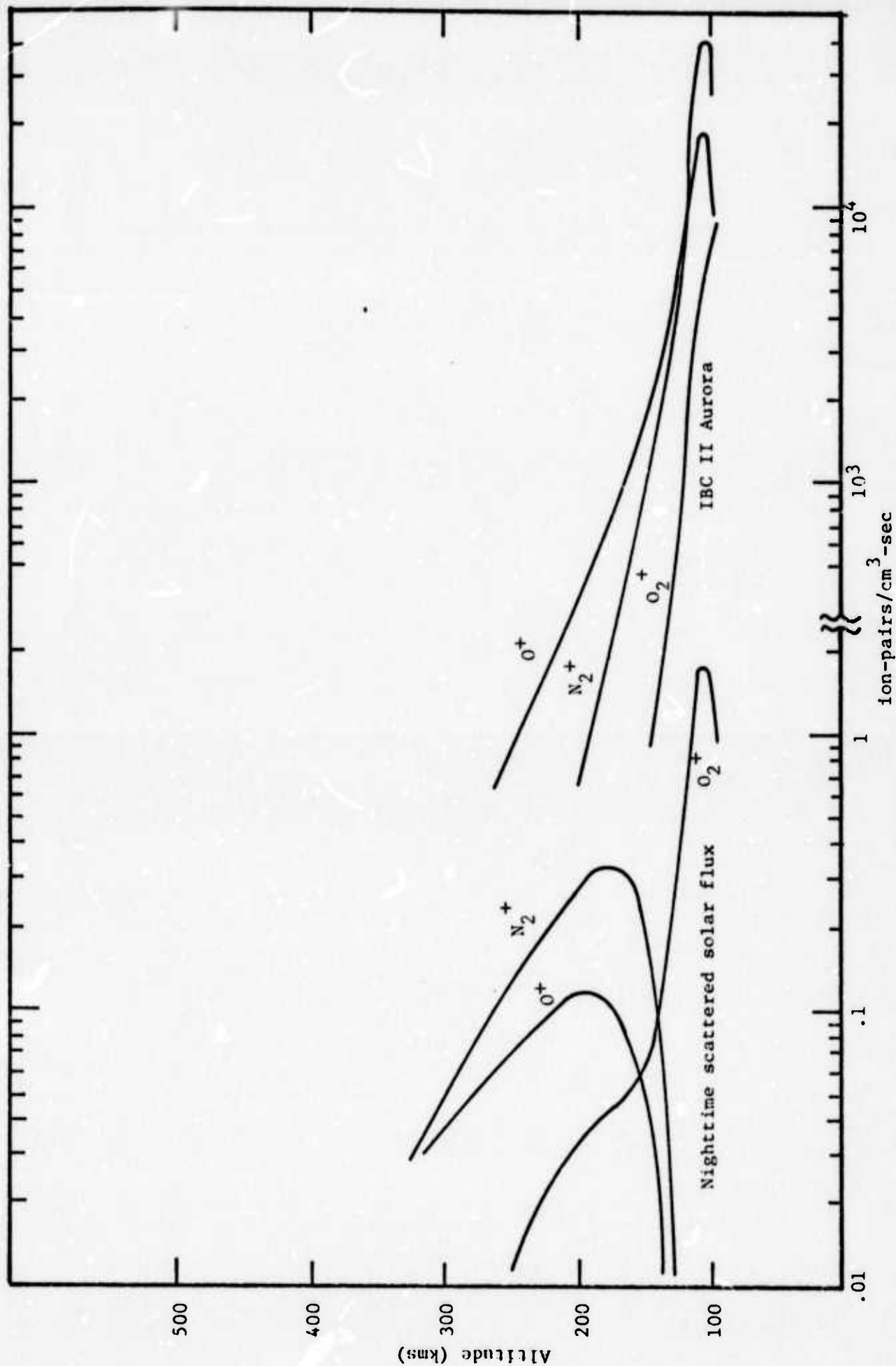


Figure 3. Ion production due to aurora electrons and nighttime scattered solar flux.

$q(h,E)$  given by Lazarev [1967] at the penetration depth  $X_m(E)$  deduced by Gerard [1970]

$$Q(h) = \int_{E_{\min}}^{\infty} q(h,E) dE \quad (\text{cm}^{-3} \text{ sec}^{-1}).$$

The ionization rate for an IBC II auroral arc is illustrated in Figure 3.

Utilizing the ionization sources, a reaction set such as given by Rees, et al, [1967], and the neutral atmosphere model of Jacchia [Jacchia, 1971], it is possible to calculate the time dependent densities of the ionic species. The computer code was very expensive to run on the Utah State University Burrough's Computers, therefore, only a limited amount of computation was actually done. Figure 4 illustrates the nighttime ionic densities at 2300 local time, 65.1N latitude, 212.5°W longitude produced by scattered radiation and drizzle flux. Also shown are ion densities after 20 minutes of an auroral described by the flux-energy diagram of Figure 5. The  $O^+$  density is excessively high at 300 km because the calculations neglected vertical transport by diffusion.

The production rates for  $N_2^+$ ,  $O_2^+$ , and  $O^+$  permit the calculation of the volumn emission rates for the Nitrogen  $3914\text{\AA}$ , the oxygen  $5577\text{\AA}$  and  $6300\text{\AA}$  radiations [Rees et al, 1967]. The  $3914\text{\AA}$  emission results from electron impact ionization and excitation of  $N_2$ . This emission is important because of the proportionality between the primary electron flux and the  $N_2^+$  production rate. The oxygen green and red



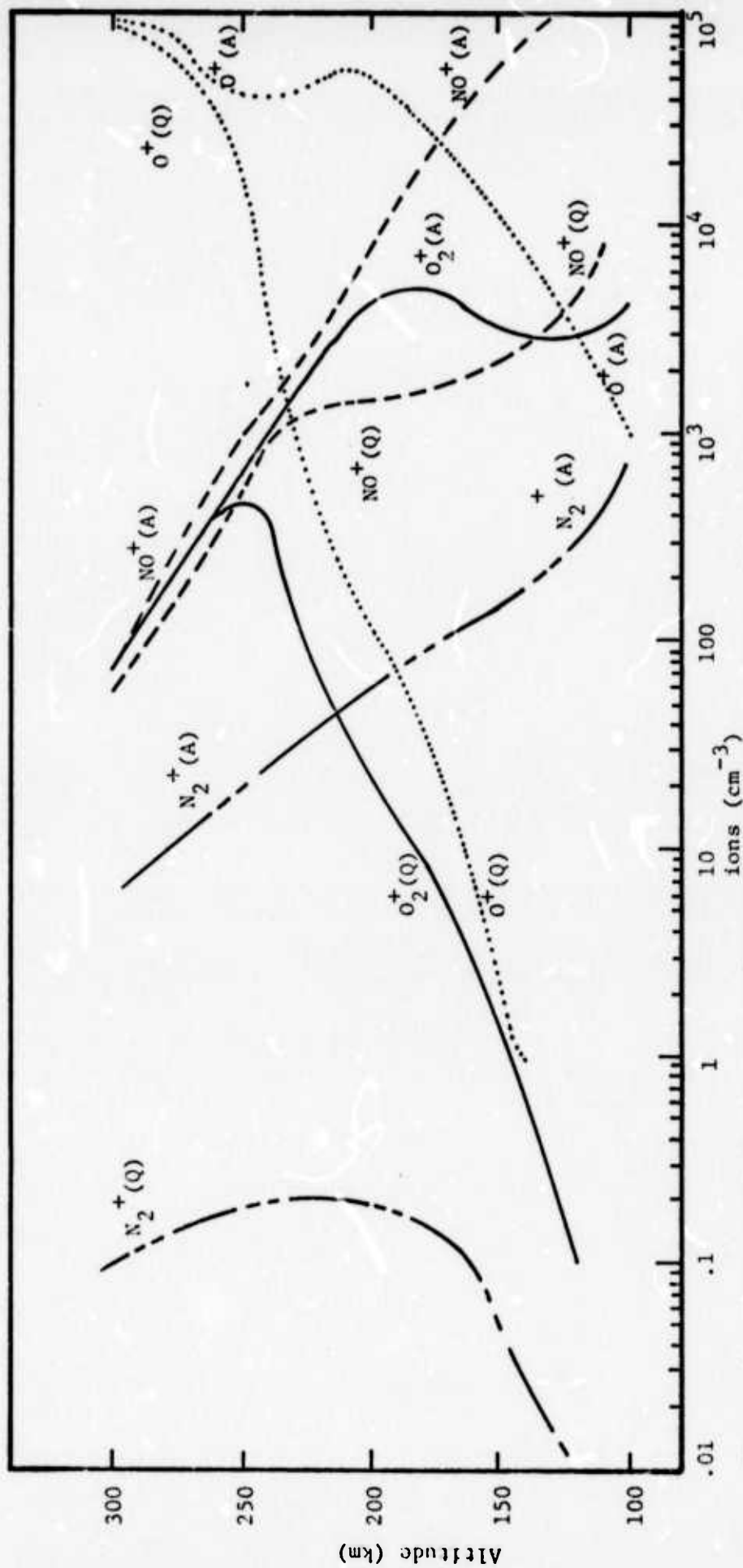
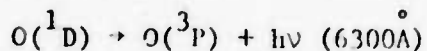
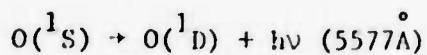


Figure 4. Theoretical ion densities for quiet (Q) and auroral arc (A) conditions.

lines are produced by the reactions.



The  $O(^1S)$  state is populated by collisional excitation of secondary electrons with oxygen atoms and also the dissociative recombination of  $O_2^+$ . The  $O(^1D)$  state is populated by collisions with the ambient electrons as well as the same excitation processes for the  $O(^1S)$  state. Our calculation of emission rates is based on the model of Rees et al, [1967], and includes collisional quenching but not diffusion. Figure 6 is a plot of the three radiation profiles for quiet and disturbed (the flux of Figure 5) conditions. This is as far as the work in this area progressed before the contract was terminated. Additional effort, funded by the University, is being made to evaluate this computer code by comparing simultaneous electron fluxes and radiation profiles which were measured by a research group at Utah State University. Copies of the completed work will be sent to the distribution list at the time of completion.

Many of the problems encountered in developing a polar ionospheric model were at the forefront of current research. Such was the case in dealing with motions produced by the collisional-heating of precipitating particles and auroral electric fields, and in simply but adequately describing the chemistry of the D region (below 100km). The Joule heating produced by auroral electric fields is of the same

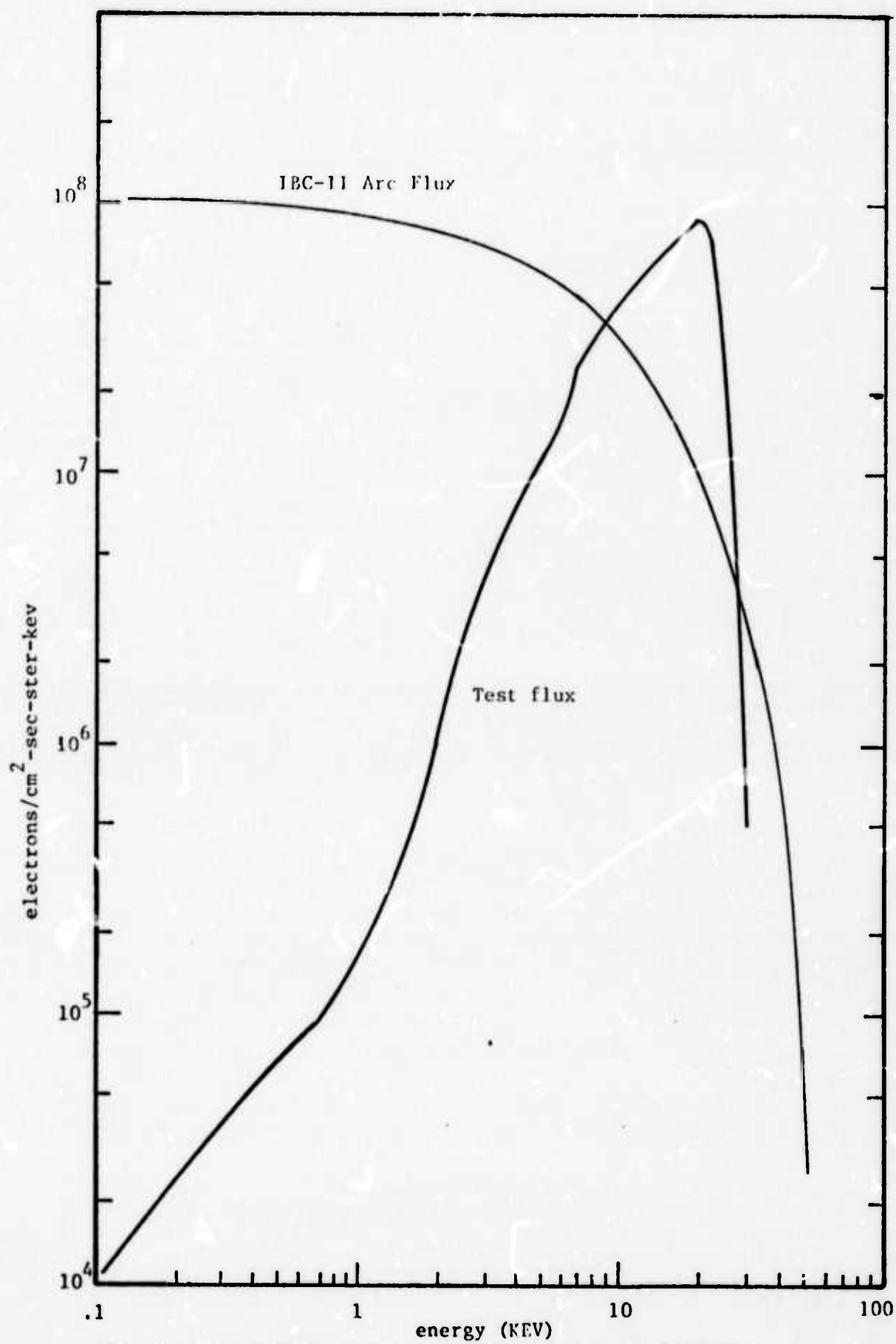


Figure 5. Auroral flux used in theoretical calculations

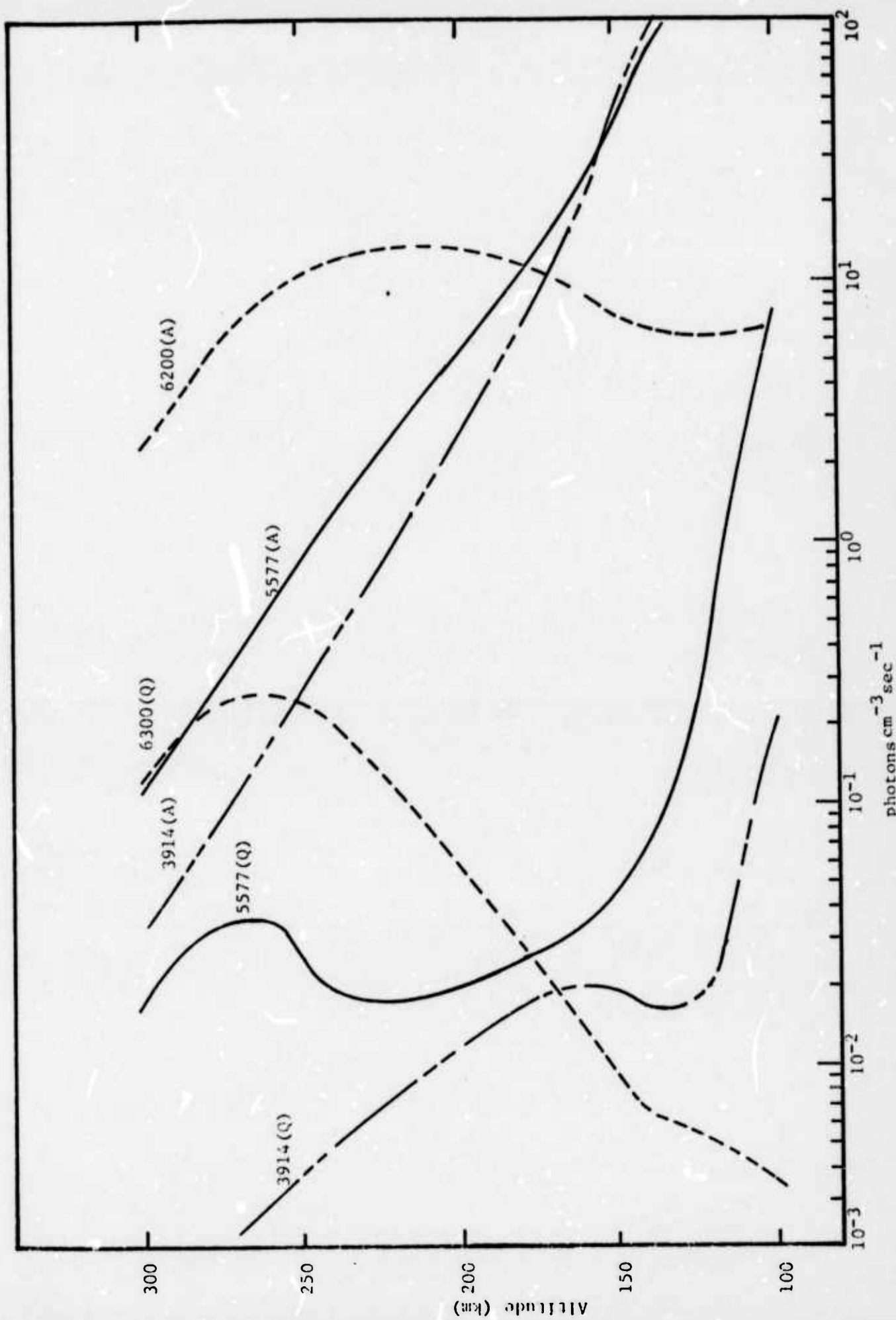


Figure 6. Volume emission profiles for quiet (Q) and auroral arc (A) conditions

order of magnitude as the solar ultraviolet heating of the thermosphere and results in an important energy source in the polar regions especially during magnetically disturbed conditions. Since the air is easily set into motion, we would expect this heating to cause large winds in the polar ionosphere. The problem of describing the auroral motion was begun by modeling a simplified 2-dimensional north-south-vertical slab of the auroral zone. Motion was caused by a north-south electric field driving ions across the geomagnetic field lines and imparting heat energy and momentum to the neutral particles through collisions. The gas equations for mass continuity, momentum and energy including viscosity and heat conduction were linearized by assuming small amplitude (perturbation) motions. A vertical pressure coordinate was employed together with the assumption of hydrostatic equilibrium. Motion in the east-west direction was calculated, but no east-west variations or pressure gradients were allowed. The neutral gas motion produced by a 50 millivolt/meter electrical field acting on a static resting atmosphere for 3-1/2 hours is illustrated in Figure 7. This important work is not completed, but Dr. Harris has received free computer time at the National Center for Atmospheric Research to make additional calculations, especially of motions about an arc. If desired, a preprint of this paper will be sent to the distribution list when available.

A complete chemical model of the D region is still under development due to the multitude of possible chemical reactions. Our philosophy for modeling this region was to utilize equivalent reaction rates that





were compatible with observed ionization features so that a predictive model could be implemented without having to evaluate the large reaction set that is in current vogue. The first problem encountered with this model was the calculation of the solar ionization and dissociation rates. We found that the NO ionization rate due to the 1027-1337 Å solar flux region had not been calculated utilizing detailed structure of either the O<sub>2</sub> absorption cross-sections or the NO ionization cross-sections. A computer subroutine, incorporating the details of the measured NO ionization cross sections [Watanabe et al, 1967], and the O<sub>2</sub> absorption cross sections [Adams, 1974], was written to evaluate ionization in this band. Results for an overhead sun are shown in Figure 8. It is seen that the hydrogen Lyman α line (1215.7 Å) produces almost an order of magnitude more ions than the 1027-1337 Å solar band. Thus, this band is only of minor importance in the D region chemistry.

The dissociation rates per molecule for CH<sub>4</sub>, CO, NO, CO<sub>2</sub>, H<sub>2</sub>O, N<sub>2</sub>O, NO<sub>2</sub>, C<sub>2</sub>H<sub>4</sub>, H<sub>2</sub>O<sub>2</sub>, O<sub>2</sub> and O<sub>3</sub> have been calculated versus altitude and zenith angle for solar wavelengths between 1000 Å and the dissociation threshold. Absorption cross sections for these species were obtained from the Joint Institute for Laboratory Astrophysics (reference library) of the University of Colorado, Boulder, Colorado. The absorbing atmosphere was assumed to be oxygen (Jacchia, 71 and U.S. Standard Atmosphere, 62) and Ozone [Adams and Megill, 1970]. These calculations are being prepared for publication in a technical journal and represent the most comprehensive and detailed description of dissociation rates available today. Figure 9, from this paper, shows the altitude where

G.A

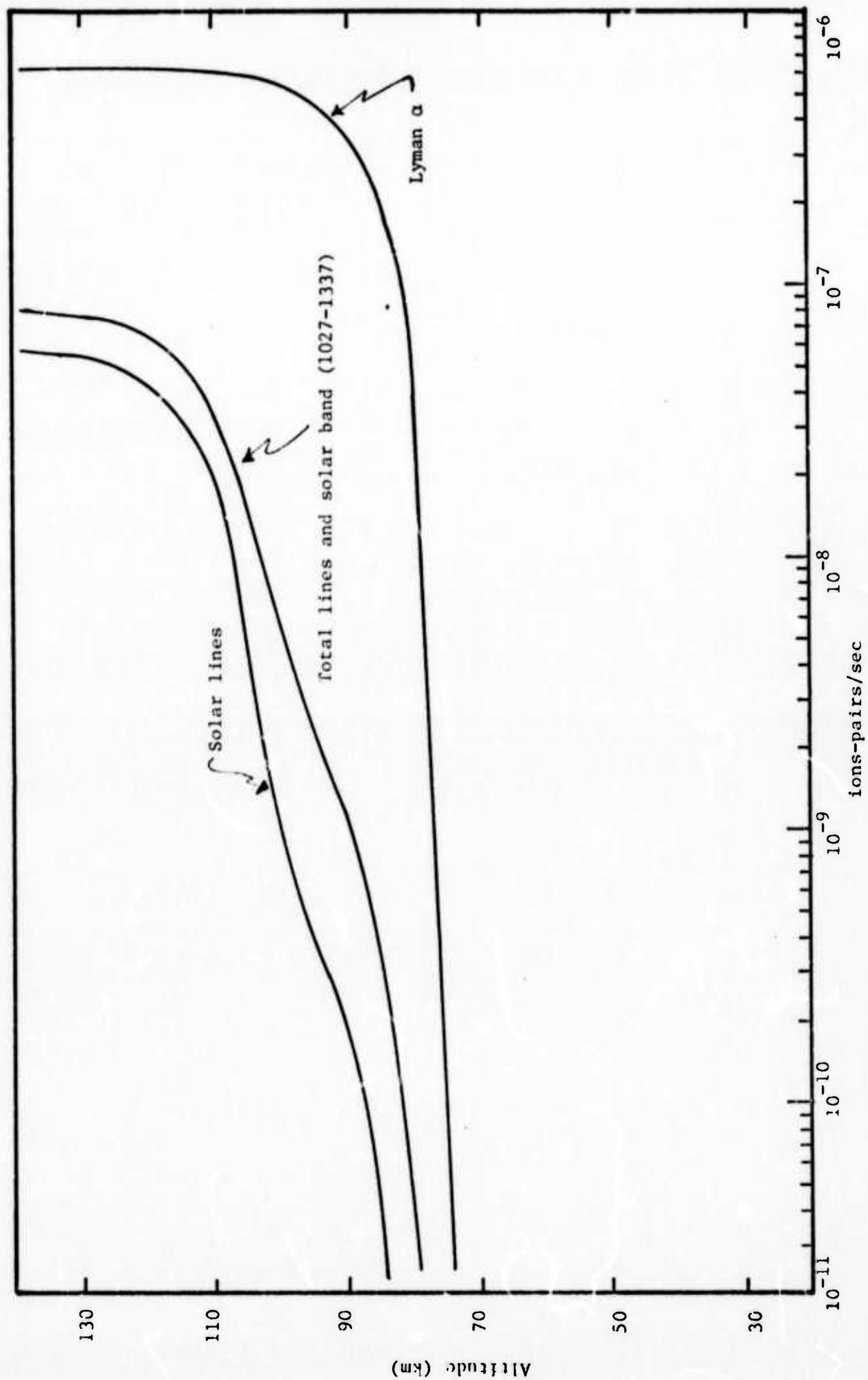


Figure 8.  $\text{NO}^+$  production rates per NO molecule.

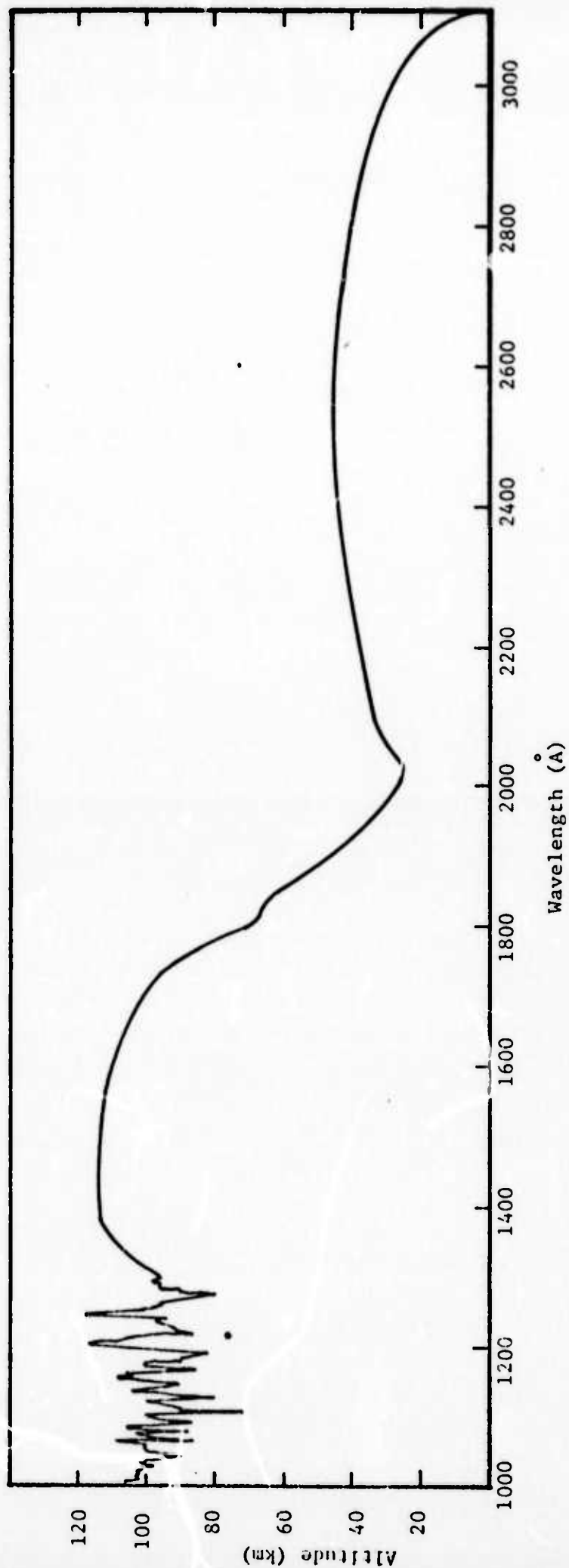


Figure 9. Altitude at which solar flux is reduced by  $e^{-1}$ .